GA–A26897

PARTICLE CONTROL AND TRANSPORT EXPERIMENTS IN THE DIII-D TOKAMAK WITH GRAPHITE WALLS

by
S.L. ALLEN, N.H. BROOKS, T. DITTMAR, R. ELLIS,
M.E. FENSTERMACHER, J.W. DAVIS, D. ELDER, B. FITZPATRICK,
A.A. HAASZ, G.L. JACKSON, A.W. LEONARD, A. LITNOVSKY,
M.A. MAHDAVI, A.G. McLEAN, T.H. OSBORNE, P.A. POLITZER,
D.L. RUDAKOV, P.C. STANGEBY, E. TSITRONE, C. TSUI,
K. UMSTADTER, E.A. UNTERBERG, W.R. WAMPLER,
W.P. WEST, D.G. WHYTE

OCTOBER 2010

GENERAL ATOMICS

DISCLAIMER

GA–A26897

PARTICLE CONTROL AND TRANSPORT EXPERIMENTS IN THE DIII-D TOKAMAK WITH GRAPHITE WALLS

by
S.L. ALLEN,[1] N.H. BROOKS, T. DITTMAR,[2] R. ELLIS,[1]
M.E. FENSTERMACHER,[1] J.W. DAVIS,[3] D. ELDER,[3] B. FITZPATRICK,[3]
A.A. HAASZ,[3] G.L. JACKSON, A.W. LEONARD, A. LITNOVSKY,[4]
M.A. MAHDAVI,[2] A.G. McLEAN,[5] T.H. OSBORNE, P.A. POLITZER,
D.L. RUDAKOV,[6] P.C. STANGEBY,[3] E. TSITRONE,[2] C. TSUI,[3]
K. UMSTADTER,[6] E.A. UNTERBERG,[5] W.R. WAMPLER,[7]
W.P. WEST, D.G. WHYTE[8]

This is a preprint of a paper to be presented at the 23rd IAEA Fusion Energy Conference, October 11–16, 2010 in Daejon, Republic of Korea and to be published in Proceedings.

[1]Lawrence Livermore National Laboratory, Livermore, California, USA
[2]Association Euratom-CEA, Institut de Recherche sur la Fusion Magnétique, CEA Cadarache, St. Paul-lez-Durance, France
[3]University of Toronto Institute for Aerospace Studies, Toronto, Ontario, Canada
[4]Institut fur Energieforschung-Plasmaphysik, Forschungszentrum Julich, Association EURATOM-FZJ, Germany
[5]Oak Ridge National Laboratory, Oak Ridge, Tennessee, USA
[6]University of California-San Diego. San Diego, California, USA
[7]Sandia National Laboratories, Albuquerque, New Mexico, USA
[8]Massachusetts Institute of Technology, Cambridge, Massachusetts, USA

Work supported in part by
the U.S. Department of Energy
under DE-AC52-07NA27344, DE-FC02-04ER54698,
DE-AC05-00OR22725, DE-FG02-07ER54917,
DE-AC04-94AL85000 and DE-FG02-04ER54762

GENERAL ATOMICS ATOMICS PROJECT 30200
OCTOBER 2010

GENERAL ATOMICS

ABSTRACT

We report new results from recent particle control and transport experiments in the DIII-D tokamak. We find that dynamic particle balance calculations (particle sources and sinks calculated vs time) yield similar results to a shot-averaged "static" (calculated by pressure rise) particle balance. The dynamic particle balance measurements show very low wall retention in both NBI- and EC- heated H-modes, compared with large retention during plasma startup. Two oxygen bakes at 1.3 kPa oxygen pressure for 2 hours at 350°C were completed and advanced inductive plasma operation was quickly recovered. No damage to tokamak internal components was observed. The removal of the hydrogenic species in DIII-D by thermo-oxidation compares well with laboratory experiments and we obtained data on thermo-oxidation of fresh ^{13}C layers in DIII-D. Particle balance in discharges with resonant magnetic perturbation (RMP) ELM suppression show that the wall retention rate and inventory is dependent on pedestal density and divertor conditions. ^{13}C injection experiments have shown that most of the carbon is deposited at the inner strike point of a SN divertor in L-mode, additional deposition in the private flux zone is present in H-mode. With an unbalanced DN plasma shape, there is more localized ^{13}C deposition near the injection point in the non-active divertor.

1. INTRODUCTION

Advanced Tokamak requirements drive the main requirements for DIII-D plasma facing components: disruption recovery before the next plasma shot and effective control of particle and power fluxes in a variety of plasma shapes. To achieve these goals, we have developed an effective combination of wall materials and conditioning: nearly all of the plasma-facing components are graphite, the wall can be baked to ~350°C before plasma operations, three divertor cryopumps provide significant particle exhaust (20 m^3/s), a variety of plasma shapes can be studied, and recovery from off-normal events is achieved between shots by glow conditioning. We find that cryopumping also affects the wall conditions by reducing the particle inventory of the wall. In all, DIII-D is a unique tokamak device for assessing the retention of hydrogenic isotopes in graphite surfaces and provides data for comparison with other experiments [1–12]. It is also important to characterize the DIII-D (wall and conditioning) configuration so that we can determine which attributes are suitable for longer pulse machines (e.g. KSTAR, EAST, JT-60SA). In the steady-state phase of burning plasma machines such as ITER, retention of hydrogenic isotopes in the first wall can lead to an unacceptable in-vessel tritium inventory [13–16].

This paper summarizes particle balance estimates performed on DIII-D with a time-dependent ("dynamic") technique and compares these results with the total pressure rise at the end of the discharge ("static" with the pumps closed, also referred to as gas balance). Dynamic particle balance measurements on DIII-D with cryopumping have been carried out for more than a decade [17–19] and the overall conclusions of the present study are consistent with the previous results. The total wall uptake from the time-integral of the dynamic measurements is within 7% of the results from the more accurate time-integrated "static" measurements. The present study's comparison of the dynamic with the static particle balance gives us more confidence in the conclusions, but also underscores the importance of time-dependent measurements. In DIII-D, the total uptake of deuterium during a plasma discharge is dominated by the wall uptake during the initial (ohmic or L-mode) part of the discharge with nearly zero uptake observed during the steady-state H-mode phase. In some cases, these measurements infer net depletion of deuterium from the wall during the H-mode phase. Since the relative duration of H-mode to L-mode can be much longer in future devices, scalings of hydrogenic (e.g. tritium) retention must be based on time-dependent particle balance or they will overestimate the retention for longer pulse machines (e.g. ITER). Cryopumping, baking, and thermo-oxidation (baking in a oxygen atmosphere) have been shown to be effective in reducing the hydrogen inventory on DIII-D. This paper presents the first thermo-oxidation of a large, high-performance tokamak; no adverse affects were observed and high performance advanced inductive "hybrid" plasma operation was achieved in less than 20 discharges.

2. PARTICLE BALANCE

Fuel retention in DIII-D is assessed with a "dynamic" particle balance calculation based on sources and sinks of a single reservoir (the DIII-D vacuum vessel), as shown in Eq. (1). The source terms are calculated from measurements: (1) gas input, (2) NBI input, and (3)neutrals; the sinks terms are: (4) Cryopump exhaust and (5) plasma density rise. Any remaining flux is attributed to the wall flux (6), where positive (negative) values imply wall retention (release). As this remainder also contains the accumulated measurement uncertainties, care must be taken in its derivation and we have utilized heating sources both with (NBI) — and without (ECH) — particle input. In the ECH case, term 2 is zero, and in the steady-state portion of the discharge, terms (3) and (5) are negligible. Note that all terms are calculated as a function of time [20].

Sources *Losses*

Gas Input (NBI Input) Neutrals Pump Exhaust Plasma Density Rise Wall Flux

$$\Gamma_{Gas}(t) + \Gamma_{NBI}(t) + \frac{dN_0(t)}{dt} - \Gamma_{Pump}(t) - \frac{d\{n_e V\}(t)}{dt} = \Gamma_{Wall}(t) \quad . \qquad (1)$$

(1) (2) (3) (4) (5) (6)

Figure 1 compares the terms in Eq. (1) for a NBI (black) and ECH (red) ELMing H-mode at the same plasma current, auxiliary input power level, and plasma shape (LSN). In the ECH case(term 2 = 0), the wall flux is obtained by the difference between the gas input (term 1) and the measured pump exhaust (term 4); the largest error is due to the measurements of the cryopump pumping speed. In the NBI case, there is an added uncertainty due to the estimates of the cold NBI streaming gas which is differentially pumped by separate NBI cryopumps. For the NBI discharges, the NBI Torus Isolation Valves (TIVs) were opened a few seconds before each discharge and then closed a few seconds after the discharge to minimize this pumping. For both heating techniques, the discharge naturally divides into two regions: a) the startup (L-mode in these discharges, t < 1000 ms) where 40 TL/s of gas is injected and the wall influx rate is large, followed by b) the steady-state H-mode period where there is negligible wall influx within the measurement uncertainties. The period of low wall flux is maintained for the length of the heating pulse and shows no indication of saturation. We do not have sufficient data to determine if the large early influx in *these* discharges is due to "startup" or L-mode, but we note that in other L-mode discharges (with no H-mode transition) there are comparably (large) wall influx rates. In Fig. 1 for the NBI case, the wall inventory is *decreasing* as a function of time after the initial startup, and we have observed cases where this integral can be negative, indicating that particles are being removed from the wall. This was also observed in a previous DIII-D study [17]. To date, however, we have not conclusively isolated the conditions for a small or negative net wall inventory, although

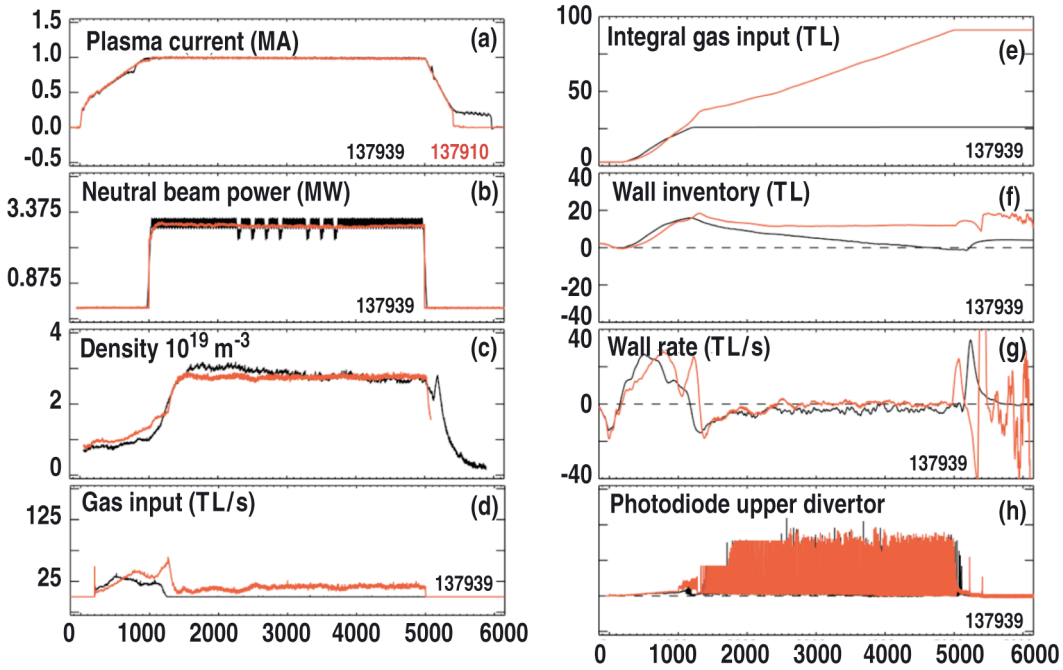

FIG. 1. ECH heated (red) H-mode plasma is compared with a NBI (black) discharge. The plasma current, neutral beam or ECH power, electron density, gas input, integral of the gas input; wall inventory and wall rate from the dynamic particle balance; along with the photodiode signal are compared with a neutral beam heated H-mode DIIID shot. Note that in both cases, the wall flux (g) is quite large in the L-mode ramp-up period, but during the ELMing H-mode, the wall flux is very close to zero.

strong cryopumping is necessary. In Fig. 2, we see a sequence of shots where the wall inventory shows an general decrease – even though it decreases/increases on four shots (note color sequence). We have not had sufficient run time to determine the longer term (~10 shot) evolution of this behavior, and it may be related to subtle details of the startup phase. However, some of the time-dependent behavior is due to the ELM characteristics of a particular shot, as the pressure rise due to the ELMs is easily seen in the time-resolved measurements of the cryopump plenum pressure – thereby modulating the pump exhaust. In the ECH case, a small ~10TL/s gas puff is required to maintain the density, indicating additional particle transport compared to the NBI case; we have not studied this trend and do not know if it is representative of all ECH H-modes. The ELM frequency in these ECH H-modes is extremely constant in time.

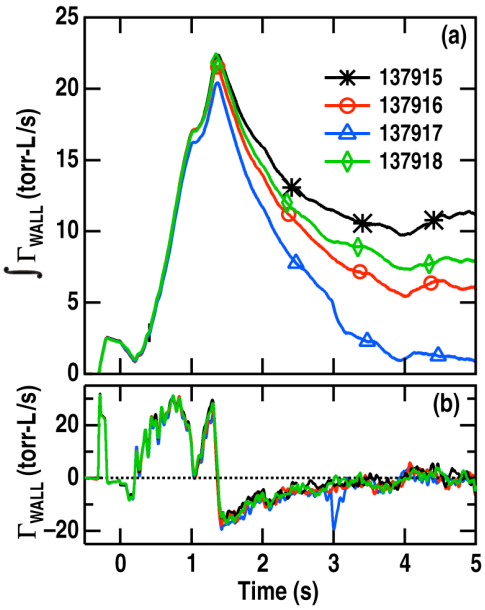

FIG. 2. Wall inventory vs. time showing a gradual decrease with time. Note the shot-to-shot variability (color code) as the shot sequence progresses.

This dynamic particle balance has now been compared with "static" particle balance measurements on DIII-D. After a series of repeat discharges, the cryopumps are warmed above LHe temperatures to release the trapped gases and the pressure rise is measured with a capacitance manometer. The product of the pressure rise with the measured DIII-D vessel volume (both with 1% uncertainty) yields a very accurate measure of the particles not retained by the wall, albeit time- and shot-integrated. This quantity can be compared with the integrated exhaust of particles from the dynamic particle balance. Measurements in ELMing H-mode, L-mode, and ohmic plasmas with cryopumping indicate that the two techniques agree to within ~10%, providing additional confidence in the dynamic technique. Shown in Fig. 3 is a detailed comparison of the two techniques during a run day. The length of the colored bars at the left of each set corresponds to the shot-integrated dynamic exhaust for each of the discharges in the set. The long blue bar at the right of each set is the static exhaust determined by the pressure rise when the cryosystem is regenerated after the set of 4 (or 3 in Set 5) discharges. The total of the dynamic exhaust for the set is within 5% of the exhaust determined by the static particle balance, providing a check on the dynamic particle balance technique.

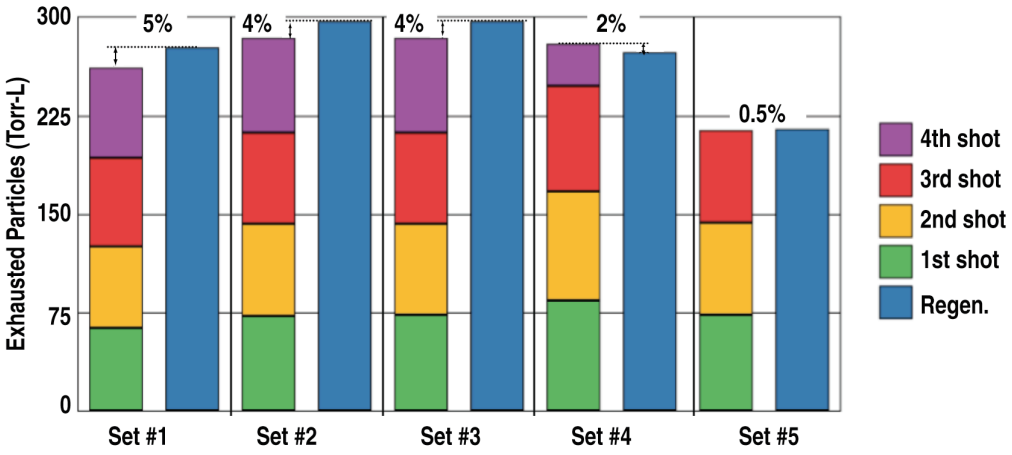

FIG. 3. Comparison of the exhausted particles for a series of discharges (y-axis). Each colored sub-block is the exhaust from a single discharge as calculated by the dynamic particle balance. The blue bar is the measurement particle released from the cryosystem by regenerating after each series of discharges.

One of the run days was preceded by a normal high temperature bake and followed by a short bake to assess the amount of hydrogen trapped in "shallow" deposits that could be removed with a 350°C bake. By "short bake" we mean that the inductive heating was stopped just after the vessel reached the 350°C bake temperature to allow sufficient cooling time for plasma operations the following day (i.e. the vessel pressure did not reach a maximum and start decreasing as in a normal bake). Starting with a "clean" wall after the normal bake, a total of ~2400 Torr-L of deuterium was injected during plasma operations. The amount exhausted was determined to be between 1010 (static) –1140 (dynamic) Torr-L. The short bake after the run day bake released an additional ~1090 Torr-L, resulting in a retained particle inventory of ~170–300 Torr-L, or ~7%–12% of the total injected particles

for this experiment. When normalized to the divertor target ion flux, this retention is <0.2%. This retention estimate is an upper bound because the operationally constrained short bake following the experiment did not return the wall to its original condition.

Dynamic particle balance measurements during resonant magnetic perturbation (RMP) ELM suppression show that the wall retention rate and inventory is dependent on pedestal density and divertor conditions [21,22]. The dominant term in the particle balance equation during RMP discharges was the cryopump exhaust rate. In a closed divertor configuration, the pump exhaust is significant throughout the ELM suppression phase. In contrast, in a more open divertor configuration, the exhaust decreased to nearly zero as the divertor transitions to a low-recycling state. It is found that the 3D magnetic field structure imposed by the RMP helps to define the magnetic geometry of the divertor, and hence the particle exhaust.

3. THERMO-OXIDATION EXPERIMENTS

To remove more deeply trapped hydrogenic layers that are co-deposited with eroded carbon in the DIII-D vessel, thermo-oxidation experiments were recently successfully completed. These techniques have been well-characterized in test chambers at the U. of Toronto [23], but the technique has had limited application in high temperature magnetic confinement devices. In preparation for an experiment on DIII-D, oxygen bake tests of internal components were carried out at U. Toronto and DIII-D test chambers to identify systems that could be damaged. Over a two year period, these tests included the cryopump components, ECH and ICH antennas, diagnostic mirrors, and other internal components [24]. The largest effect was found on copper surfaces as they would receive an oxide coating. These laboratory experiments were used to determine the parameters for the DIII-D thermo-oxidation experiment, which was a compromise between minimizing the risk to components and optimizing the removal rate of hydrogenic species. Using these optimized parameters, two thermo-oxidation experiments were carried out on DIII-D; each was a 2 hour bake at 350°C in a 80%/20% Helium/Oxygen (similar to Heliox) atmosphere at 1.3 kPa.

The goals of the first thermo-oxidation bake were to test recovery of plasma operations, assess removal of ^{13}C from a few DIII-D tiles that had been characterized in previous ^{13}C experiments, and expose other special samples (e.g., thick co-deposits from Tore-Supra and stainless steel buttons to look for carbon migration). Before the first bake, specially prepared samples on stalks were inserted into the vacuum vessel during a “clean” (no personnel entry) vent. DIII-D operational experience is that plasma operations are quickly recovered after this type of vent with a 350°C bake. After the samples were installed, the machine was heated to 350°C, the turbomolecular pumps were closed, and the vessel pressure was raised to 1.3 kPa with the Heliox gas. Because of high thermal conductivity of helium, the heating of in-vessel components was nearly uniform. A constant temperature was maintained by slightly increasing the inductive heating to offset the increased thermal transport of the higher pressure; thermocouples attached very close to the samples monitored their temperature. During the first ~90 minutes of the bake, we saw a 6x decrease in the 32 amu peak (mostly O_2) and a large increase in the 44 amu (mostly CO_2) RGA peak, similar to that observed in the tests at U. of Toronto, and indicating that thermo-oxidation was taking place. To ensure that there was sufficient oxygen for the thermo-oxidation reaction, we then pumped and backfilled the vessel again to 1.3 kPa with fresh Heliox for the final 30 minutes. After machine cool down (about 1 day), a clean vent was again used to remove the samples and the machine was baked. Before plasma operations, both the ECH and FW heating systems were successfully tested; the FW antenna voltage loading was slightly better than before the therm-oxidation. Visual inspection of copper samples on the stalks showed slightly less oxidation than observed in the small vessel tests. After the second thermo-oxidation, the pumping speed of the cryopumps was re-measured as a function of pressure, both to assess if there were any changes caused by the thermo-oxidation experiments and to check the values used for the

particle balance experiments. The speed tests showed no differences within the measurement uncertainties, and the pump cooling times and He flow rates were unchanged. A detailed in-vessel inspection was carried out at the end of the experiment, and there was no damage that could be attributed to the thermo-oxidation experiment.

Initial results on the effectiveness of the DIII-D thermo-oxidation experiments are shown in Fig. 4. The solid line is the fraction of D remaining as a function of time for a DIII-D tile undergoing thermo-oxidation with the standard parameters as measured by the laboratory experiments at U. of Toronto. The single red point is the average difference measured before and after the DIII-D experiments from one of the stalk-mounted tiles as measured by Nuclear Reaction Analysis. DIII-D tiles with known D content were used for the data shown in Fig. 4. Excellent agreement is seen between the laboratory and DIII-D experiments, indicating that laboratory results can be used to estimate hydrogenic removal rates in DIII-D.

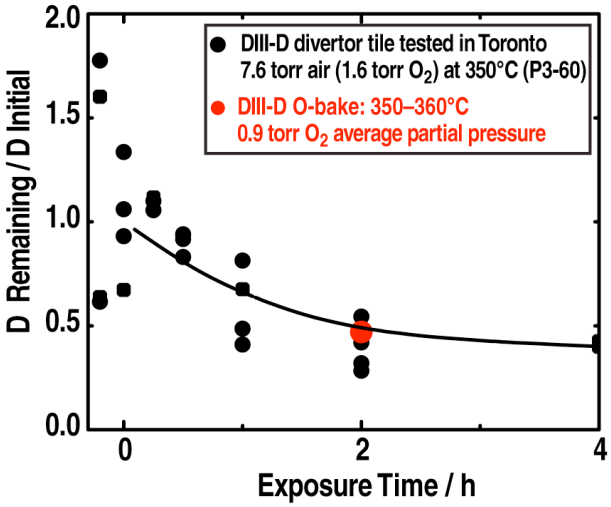

FIG. 4. Thermo-oxidation removal of fractional deuterium content for a DIII-D tile in the Toronto facility (line) as a function of time compared with the measured average of a tile after the 2 hour DIII-D thermo-oxidation experiment (red point).

Plasma recovery after the thermo-oxidation was similar to or slightly better than recovery from a clean vent. Ohmic plasma operation was obtained on the very first attempt (142760), and high performance advanced inductive "hybrid" operation was obtained in about 15 shots. As shown in Fig. 5, confinement parameters such as H_{98y2} and β_N quickly returned to levels comparable with the DIII-D reference shot. The DIII-D "hybrid" or advanced inductive shot is a standard discharge carried out at intervals during the DIII-D run campaign to assess relative performance and wall conditions. The database of these shots contains impurity and radiated power trends, and these post thermo-oxidation discharges had an elevated oxygen level, as seen in Fig. 5. Continued plasma operation and an extended bake reduced the oxygen levels, but they did not decrease to the level of the reference shot. However, these elevated oxygen levels did not significantly affect the discharge performance. Because of time constraints, a boronization was not carried out, which always dramatically reduces the DIII-D oxygen levels. While the first thermo-oxidation experiment on DIII-D was to assess plasma

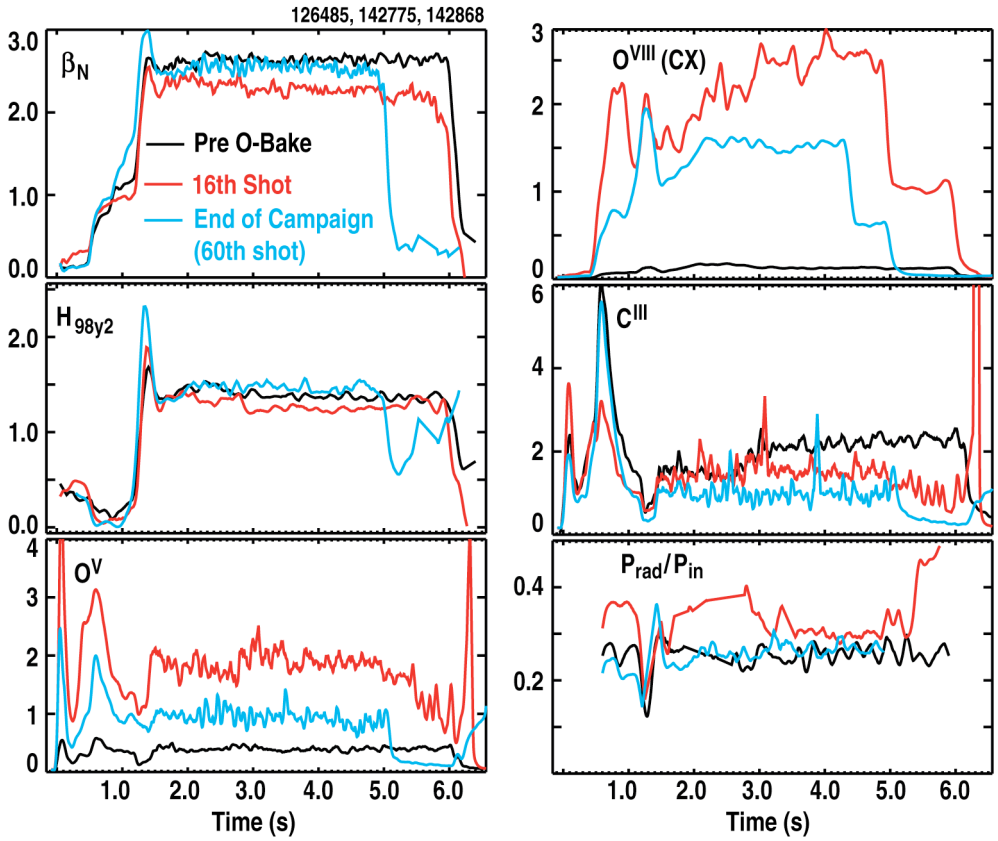

FIG. 5. The DIII-D conditions of the standard advanced inductive (black) discharge (before the thermo-oxidation bake) were quickly recovered after the bake (red); the 16th shot is shown. The elevated oxygen levels gradually decreased with subsequent shots (light blue) and additional baking.

recovery and D removal on a small number of tiles that had previously had ^{13}C deposition, the goal of the second experiment was to measure the change on a larger number of tiles and to test fresh deposits – i.e. ^{13}C deposits that had not been exposed to air and water vapor. Since 2004, DIII-D has done a series of ^{13}C deposition experiments that involve the toroidally symmetric injection of ^{13}C into a series of (typically ~15) discharges at the end of a run campaign, followed by removal of tiles during a vent and subsequent analysis to determine the regions of high deposition [25]. Injection into the "crown" of a single-null divertor plasma in L-mode (2004) showed that the highest concentration of ^{13}C was at the inner strike point in the lower divertor. For ELMing H-mode plasmas (2006), the deposition extended into the private flux region, presumably due to particle transport in the divertor by ELMs. As shown in Fig. 6, in 2008, when ^{13}C

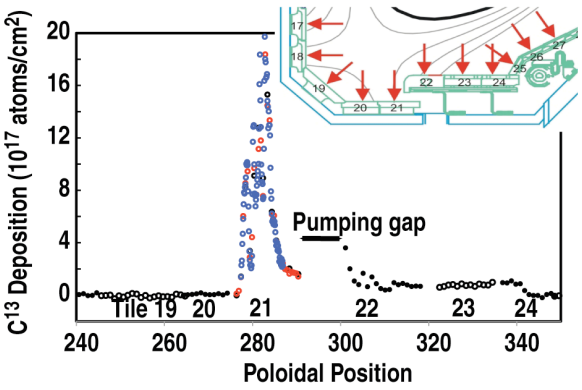

FIG. 6. ^{13}C density as a function of position for injection into the lower divertor (2008) of a LSN plasma. The second thermo-oxidation experiment used this same configuration for deposition and tiles were removed for analysis.

was the injected into the crown of an unbalanced double null plasma (drsep ~2), we measure more ^{13}C deposition near the injection point (i.e. opposite the main divertor). This plasma configuration is simulating the wall interaction near the secondary divertor in a USN plasma which may have less armor than the primary divertor (e.g. ITER). Before the second thermo-oxidation experiment, plasma conditions similar to those used in the data of Fig. 6 were established, and these were followed by a sequence of 15 identical shots with ^{13}C injection. This established a fresh pattern of ^{13}C that should be similar to Fig. 6. The second thermo-oxidation was carried out with the same parameters as the first, although it was not thought necessary to refill the vessel after 90 minutes to replenish the oxygen as in the first attempt. During both thermo-oxidation experiments, the RGA showed similar results. In addition, a new diagnostic based on measurements of IR molecular absorption with a high resolution FTIR spectrometer was commissioned. A IR source was directed through the CO_2 interferometer path resulting in a path of several meters through the vacuum vessel. IR absorption in the 400–3600 cm^{-1} region allowed measurement of the time histories of CO, CO_2, and D_2O without the ambiguity inherent in RGA spectra (i.e. multiple species cause signal at a particular amu). After the second thermo-oxidation, a total of 24 tiles were removed and are being analyzed at Sandia National Laboratory.

4. SUMMARY

These experiments show the importance of dynamic particle balance measurements on DIII-D because the influx to the wall is nearly zero during the H-mode phase. Shot-integrated (static pressure rise) ~20% wall influx measurements are dominated by the early phase of the discharge. In future machines, where the H-mode period will be an even greater fraction of the discharge time, using the static values (~20%) can result in a significant over-estimate of the wall inventory. For removing Deuterium that is co-deposited with carbon, we find that the removal rates in the DIII-D tokamak are consistent with measurements in the lab. No tokamak systems were damaged by the oxygen bake, but copper surfaces must be handled carefully. High performance advanced inductive operation in DIII-D is quickly recovered after the thermo-oxidation, albeit with elevated oxygen levels.

REFERENCES

[1] LOARER, T., et al., J. Nucl. Mater. **390-391**, 20 (2009).

[2] LOARER, T. et al., Nucl. Fusion **47**, 1112 (2007).

[3] LOARER, T. et al., "Overview of Gas Balance in Plasma Fusion Devices," Fusion Energy 2004 (Proc. 20th Int. Conf. Villamoura, Portugal 2004) http://www-naweb.iaea.org/napc/physics/fec/fec2004/datasets/EX_P5-22.html

[4] TSITRONE, E., et al., J. Nucl. Mater. **363**, 12 (2007).

[5] TSITRONE, E., et al., J. Nucl. Mater. **337**, 539 (2005).

[6] BUCALOSSI, J., et al., J. Nucl. Mater. **363**, 759 (2007).

[7] ROHDE, V., et al., Nucl. Fusion **49**, 085031 (2009).

[8] NAKANO, T., et al., Nucl. Fusion **48**, 085002 (2008).

[9] NAKANO, T., et al., J. Nucl. Mater. **363-365**, 1315 (2007).

[10] ASAKURA, N., et al., Plasma Phys. Control. Fusion **46**, B335 (2004).

[11] MAYER, M., et al., Nucl. Fusion **47**, 1607 (2007).

[12] KUBO, H., et al., "Particle Control Under Wall Saturation in Long-pulse High Density H-mode Plasmas of JT-60," Fusion Energy 2006 (Proc. 21st Int. Conf. Chandu, 2006), http://www-pub.iaea.org/MTCD/Meetings/fec2006pp.asp, paper EX/P4-11.

[13] LIPSCHULTZ, B., et al., Nucl. Fusion **47**, 1189 (2007).

[14] LOARTE, A., et al., Nucl. Fusion **47**, S203 (2007).

[15] ROTH, J., et al., J. Nucl. Mater. **390**, 1 (2009).

[16] ROTH, J., et al., Plasma Phys. Control Fusion **50**, 103001 (2008).

[17] MAINGI, R., et al., Nucl. Fusion **36**, 245 (1996).

[18] ALLEN, S., et al., Plasma Phys. Control. Fusion **37**, A191 (1995).

[19] MAHDAVI, M.A., et al., Controlled Fusion and Plasma Physics (Proc. 22nd Eur. Conf. Bournemouth, 1995), Vol. 17C, European Physical Society, Geneva (1995) 647

[20] UNTERBERG, E.A., et al., "Global particle balance measurements in the all graphite first wall DIII-D tokamak during ELM-y and RMP ELM suppressed H-mode discharges," submitted to J. Nucl. Mater., 2010.

[21] UNTERBERG, E.A., et al., Nucl. Fusion **49**, 034011 (2010).

[22] UNTERBERG, E.A., et al., Nucl. Fusion **49**, 092001 (2009).

[23] DAVIS, J.W., and HAASZ, A.A., J. Nucl. Mater. **390-391**, 532 (2009).

[24] FITZPATRICK, B.W.N., et al., "Assessment of collateral effects of thermo-oxidation on in-vessel DIII-D components in preparation for performing in-situ oxidation in DIII-D," Fusion Sci. Technol., 2010 (in press).

[25] ALLEN, S.L., et al., Fusion Energy 2006 (Proc. 21st Int. Conf. Chandu, 2006), http://www-pub.iaea.org/MTCD/Meetings/fec2006pp.asp, paper EX/P4-1; see also W.R Wampler, et al., J. Nucl. Mater. **363**, 72 (2007).

ACKNOWLEDGMENT

This work was supported in part by the U.S. Department of Energy under DE-AC52-07NA27344, DE-FC02-04ER54698, DE-AC05-00OR22725, DE-FG02-07ER54917, DE-AC04-94AL85000 and DE-FG02-04ER54762and work performed at U. Toronto was funded by the Natural Sciences and Engineering Research Council of Canada.